



Photonic crystal fiber Fabry–Perot interferometer for humidity sensor

Namaa Salem Rahim¹ · Sudad S. Al-Bassam¹

Received: 23 May 2023 / Accepted: 23 June 2023
© The Author(s), under exclusive licence to The Optical Society of India 2024

Abstract This work designed and implemented of photonic crystal fiber Fabry–Perot interferometer based on (SPR) technology for sensing the humidity of the environment. The FPI was created by directly splicing a short length of PCF (4 cm) solid core on one side with traditional multi-mode fiber (MMF) and depositing a nano-film of gold with a thickness of 40 nm on the end of the PCF sensor. The PCF–SPR experiment was observed for different degrees of relative humidity. The location of the resonant wavelength peaks is seen to change to longer wavelengths (redshift) as (the RH) increases due to the transmission of maximum energy from the reflected power of the light guided via the fiber to the surface plasmons. The calculated sensitivity, signal-to-noise ratio, figures of merit, and resolution are approaching; the S is 1.25 nm/%RH, SNR is 0.0066, the resolution is 0.08, and the FOM is 0.00083 for photonic crystal fiber.

Keywords Fabry–Perot interferometer (FPI) · Humidity sensor · Photonic crystal fiber · Surface plasmon resonance · Optical fiber sensor

Introduction

Optical fiber-based sensing technology includes performed escalating attention due to its many advantages over traditional sensing technologies. Close size, comfortable fabrication, flexibility, and more steady comeback are the main benefits of optical fiber sensors. Moreover, they are resistant

to electromagnetic interference and can efficiently be established for structural health monitoring in dangerous atmospheres and remote regions. The optical fiber sensors can furthermore be integrated with the laboratory on chip-based instruments and difficult sensing networks [1]. (PCFs) are a distinct kind of optical fiber featured via periodic micro-capillary structures. PCF is an optical produced excellent characteristic over standard optical threads in addition a good geometry over traditional optical fiber. It contains important features, for instance, smallish size, unrestricted from electrical impedance, geometric adaptability, enhanced affectability, and consecrated parallel concerning fiber optic media communications making it great for opto-gadgets [2]. In modern years, PCFs have obtained an excellent deal of research concentration in sensing performances [3]. Corresponded with the optical fiber, PCF includes a diffusion of air gaps in the cladding area, stretching infinitely along the fiber axis, and it includes an elastic design and several wonderful possessions, comprising endless single mode, heightened nonlinearity, elevated birefringence, enormous mode field size, mitigation of plugging material, lower information losing, manageable diffusion, and so on [4–6]. Photonic crystal fibers (PCFs) [7, 8], furthermore named holey fibers or microstructured optical fibers, are formed of a periodical array of air holes driving along their whole length and containing light in the imperfections of the periodic form, contain unique possessions corresponding to traditional optical fibers like unusual chromatic dispersion, high birefringence, etc. In addition, the optical possessions of silica-air PCFs are determined by the place, dimension, and form of the air holes, and can be stretched by plugging the holes with materials, for example, liquid crystals [9], semiconductors [10], or metals [11, 12], therefore have several benefits for sensing uses.

✉ Namaa Salem Rahim
namaasalem652@gmail.com

¹ Department of Physics, College of Science, University of Baghdad, Baghdad, Iraq

Surface plasmon resonance is an optical phenomenon described as the collaborative oscillation of unrestrained electrons on the edge between the dielectric and metal stimulated by an electromagnetic wave and can be excited by the electron or photon [13]. When the wave vector of the surface plasmon equals the wave vector of the incident field, there is an abrupt dip in reflected intensity and this phenomenon is named (SPR) [14, 17]. (PCF) sensor based on (SPR) has been widely applied in the areas of component content sensing [18], environmental monitoring [19], and medical treatment [20] since it has excellent advantages of simple structure, small volume, high sensitivity, real-time detection, rapid response, and anti-interference [21]. The discovery of relative humidity (RH) utilizing optical fiber, such as a sensing platform, comprising evanescent wave sensors [22, 23], and Fabry–Perot (FP) interferometers [24, 25], has been reported. The expansion of optical fiber for humidity sensing offers many benefits: impunity to electromagnetic interference and secure process in the flammable or explosive environment, in addition to miniature size, the feasibility of multiplexing the data from different sensors in the same optical fiber, and the potential of remote sensing and continued monitoring in restricted or dangerous environments [25]. This work included the manufacture and implementation of photonic crystal fiber (ESM-12) covered with a light layer of Au (40 nm) as the sensing segment based on surface plasmon resonance for sensing and measuring the relative humidity (RH) of the environment.

Fabry–Perot interferometer

FPI usually consists of two similar reflecting surfaces split by a specific space [25]. Occasionally it is named an etalon [26]. When the numerous superposition of the reflected and the transmitted rays at two similar surfaces Interference occurs [27]. The FPI can be easily designed by deliberately making up reflectors inside or outside of fibers. FPI sensors can be generally categorized into two types: extrinsic and intrinsic as in Fig. 1. [28, 29]. The intrinsic FPI fiber sensors require reflecting elements inside the fiber itself. The regional hollow of the intrinsic FPI can be designed by many of techniques, for example, thin film deposition as in Fig. 2 [30, 31], chemical etching [32, 33], and fiber Bragg gratings (FBGs) [34, 35].

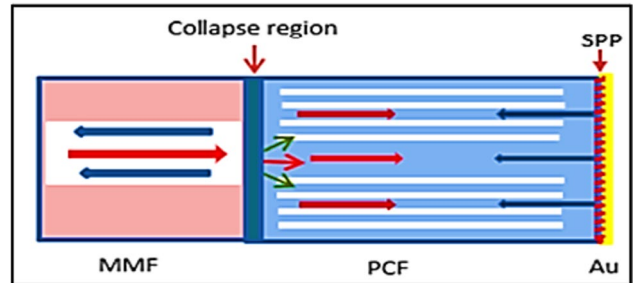


Fig. 2 The diagram of the MMF–PCF based on the SPR sensor

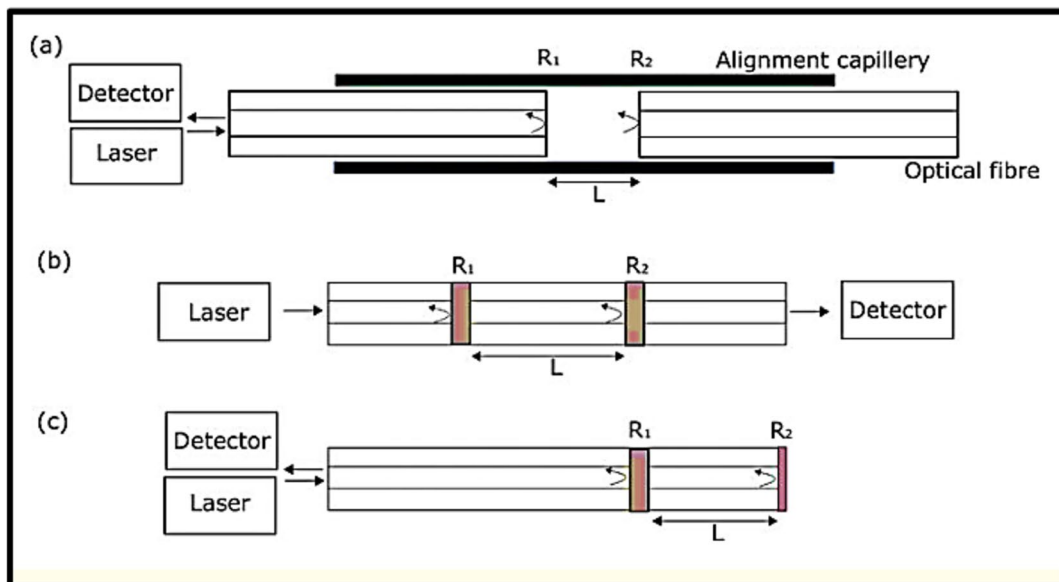
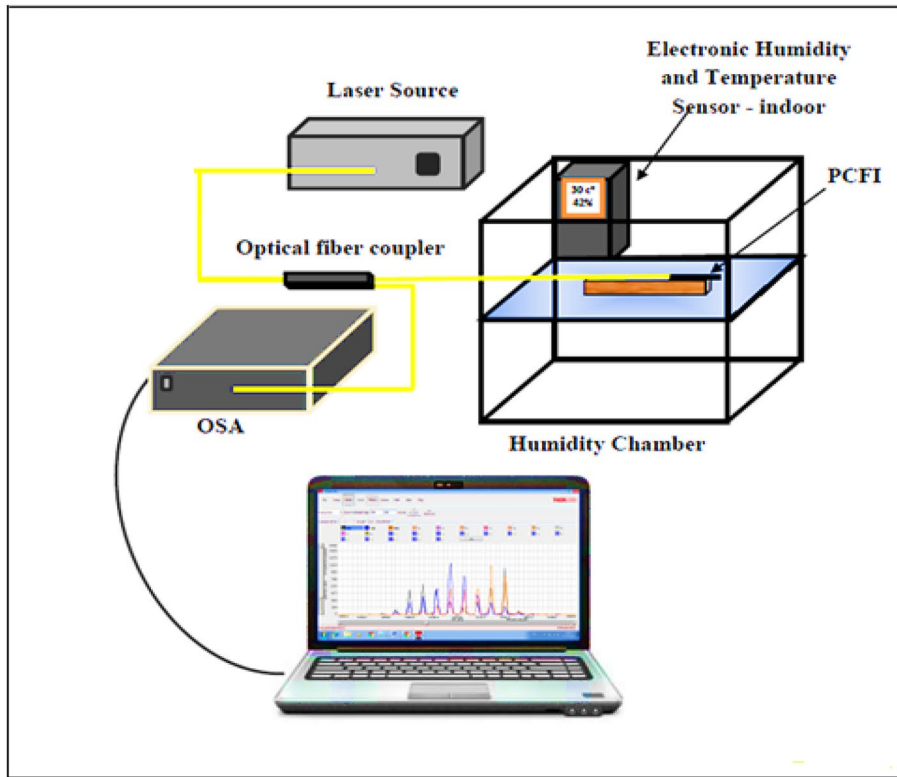
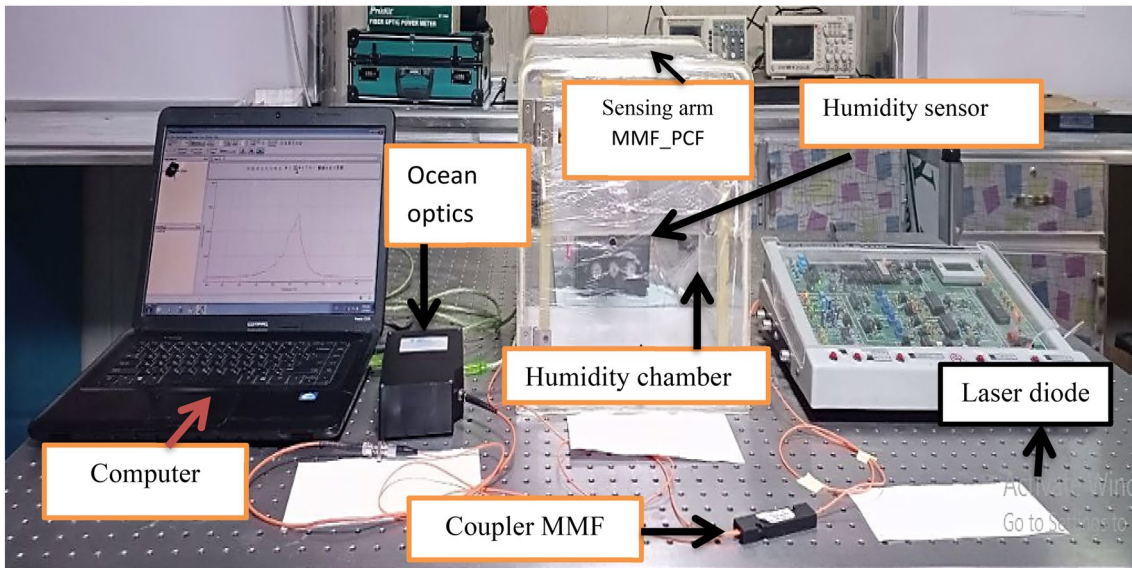


Fig. 1 **a** The diagram of an extrinsic FPI; **b** the diagram of an intrinsic Fabry–Perot interferometer; **c** the diagram of an intrinsic FPI employed in reflection mode. R_i denotes the reflective surfaces, and L is the length of the hollow [38]



(a)

PI



(b)

Fig. 3 **a** The outline of the practical design of SPR based on photonic crystal fiber Fabry–Perot interferometer sensor. **b** Photograph of experimental setup of SPR based on photonic crystal fiber FPI sensor

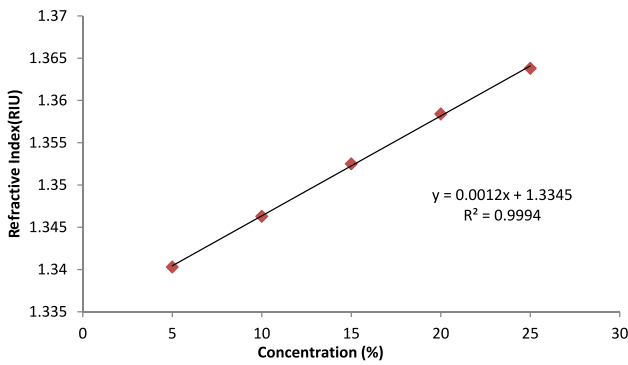


Fig. 4 PCF-SPR calibration curve using sucrose/water solution

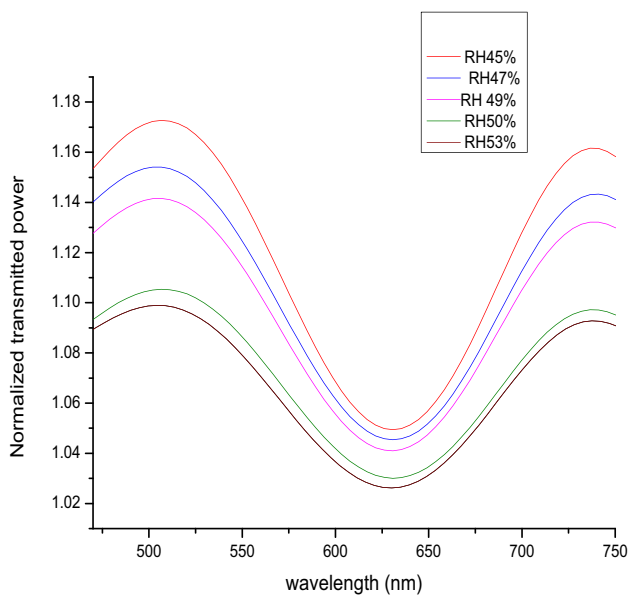


Fig. 5 SPR curve of the PCF with Au metal for different relative humidities (RH%)

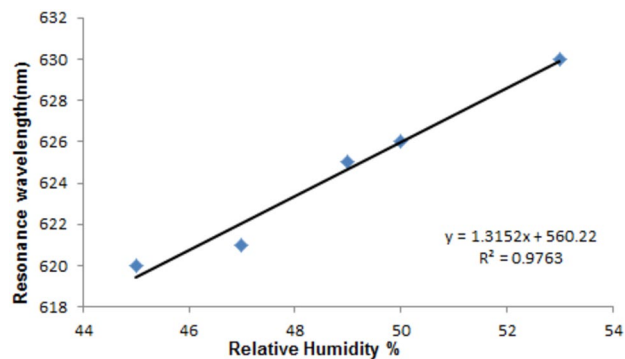


Fig. 6 Resonance wavelength λ_{res} as a function of relative humidity (RH%) for a gold-coated layer

Table 1 Performance parameters of gold layer

Metal/ (thickness)	Sensitivity (nm/%RH)	Figure of merit (FOM)	Signal-to-noise ratio (SNR)	Resolution
Gold/ (40 nm)	1.25	0.00083	0.0066	0.08

Table 2 Relative humidity (RH%) values for various resonance wavelengths λ_{res} (nm)

Type of fiber	Resonance wavelength λ_{res} (nm)	Relative humidity (RH%)
PCF	620	45
	621	47
	625	49
	626	50
	630	53

The performance parameter of photonic crystal fiber sensor

Quality factors to be calculated include sensitivity, resolution, figure of merit, and signal-to-noise ratio. Sensitivity is definite such as the variation in resonance wavelength per unit change in relative humidity of the sensing medium, and it can be written as [13]:

$$S = \frac{\Delta\lambda_{res}}{\Delta RH} \tag{1}$$

The resolution is definite as the minimum of variation in relative humidity that is measurable through the sensor, and then is given as [13]:

$$R = \frac{\Delta RH}{\Delta\lambda_{res}} \cdot \Delta\lambda_{DR} \tag{2}$$

($\Delta\lambda_{DR}$) is the spectral resolution of the spectrometer.

(SNR) and (FOM) are inversely proportional to the width of SPR spectral curve and can be written as [13]

$$SNR(n) = \left[\frac{\Delta\lambda_{res}}{\Delta\lambda_{0.5}} \right] \tag{3}$$

where $\Delta\lambda_{0.5}$ is the width of the spectral curve

$$FOM = \frac{S}{\Delta\lambda_{0.5}} \tag{4}$$

Experimental work

The outline demonstrates the segments of the SPR-based photonic crystal fiber Fabry–Perot interferometer sensor design indicated in Fig. 3a. In the case of MMF–PCF, it is mainly divided into four components: a light beam produced by a laser diode with a wavelength of 632 nm with power 0.05mW, PCF (ESM-12) (Thorlabs Co.), Multi_Mode Fiber, coupler, a computer-connected spectrophotometer (HR4000CG UV-NIR), and finally a humidity chamber with a humidity sensor (wireless sensor) from Mebus putting inside chamber. Humidity was generated through a simple electrical device placed inside a chamber containing a humidity sensor for measuring humidity. Figure 3b shows an image of the experimental setup.

The results and discussion

By immersing the coated end surface of PCF in various sucrose solutions and calculating the solutions' refractive indices, the performance of the sensor is calculated. The calibration curve for PCF and also the line connection between RI and solution concentration are shown in Fig. 4.

Using a 5-cm-long photonic crystal fiber sensor and a PCF diameter (D) of 125 μm , a coated metal layer thickness of 40 nm, the sensing process was finished. Figure 5 illustrates how the resonance wavelength suddenly increase and shift in the direction of longer wavelengths (redshift) after the humidity of the environment inside the chamber increases. The spectrum is created by the use of an optical cable to capture light curves. The optical signal intensity (I_0) obtained without any effect of humidity (sensing area) is divided by the intensity (I) measured with a humidity effect to determine the transmission (sensing medium). One option is to utilize the transmission as a function of wavelength (nm). The surface plasmon resonance curvature is referred to as the resonance wavelength. The wavelength shift and relative humidity sensor all follow a constant curve relationship. Figure 6 illustrates plasmon resonance curves at various relative humidities (sensing medium). Table 1 illustrates the performance characteristics values for the sensor using the Au coating, where sensitivity, resolution, figure of merit, and signal-to-noise ratio were computed. Table 2 explains the values of resonance wavelength and values of relative humidity (RH%).

Conclusion

This research presents a reflection-type sensor (PCF) based on SPR technology to be exploited for sensing relative

humidity. From the results, we conclude that the value of the resonant wavelength differs with the value of relative humidity (RH%). The resonance wavelength rises due to a growth in (RH). The results show that photonic optical fiber based on SPR sensing with a 40 nm thickness gold metal layer and 4 cm of exposed sensing region achieves effective performance parameters for PCF such as sensitivity reaching 1.25 nm/RH%, SNR 0.0066, FOM 0.00083, and R is 0.08.

References

1. H.H. Qazi, S.F. Memon, M.M. Ali, M.S. Irshad, S.A. Ehsan, M.R.B. Salim, M. Idrees, Surface roughness and the sensitivity of D-shaped optical fibre sensors. *J. Mod. Opt.* **66**(11), 1244–1251 (2019)
2. H. Ademgil, S. Haxha, PCF based sensor with high sensitivity, high birefringence and low confinement losses for liquid analyte sensing applications. *Sensors* **15**(12), 31833–31842 (2015)
3. H. Ademgil, S. Haxha, Highly birefringent nonlinear PCF for optical sensing of analytes in aqueous solutions. *Optik* **127**(16), 6653–6660 (2016)
4. J. Yang, L. Zhou, X. Che, J. Huang, X. Li, W. Chen, Photonic crystal fiber methane sensor based on modal interference with an ultraviolet curable fluoro-siloxane nano-film incorporating cryptophane A. *Sens. Actuators B Chem.* **235**, 717–722 (2016)
5. T. Cheng, Z. Duan, M. Liao, W. Gao, D. Deng, T. Suzuki, Y. Ohishi, A simple all-solid tellurite microstructured optical fiber. *Opt. Express* **21**(3), 3318–3323 (2013)
6. W.C. Wong, C.C. Chan, L.H. Chen, T. Li, K.X. Lee, K.C. Leong, Polyvinyl alcohol coated photonic crystal optical fiber sensor for humidity measurement. *Sens. Actuators B Chem.* **174**, 563–569 (2012)
7. P. Russell, Photonic crystal fibers. *Science* **299**(5605), 358–362 (2003)
8. P. Russell, Photonic-crystal fibers. *J. Light Wave Technol.* **24**(12), 4729–4749 (2006)
9. D. Noordegraaf, L. Scolari, J. Lægsgaard, T.T. Alkeskjold, G. Tartarini, E. Borelli, S.T. Wu, Avoided-crossing-based liquid-crystal photonic-bandgap notch filter. *Opt. Lett.* **33**(9), 986–988 (2008)
10. H.K. Tyagi, M.A. Schmidt, L.P. Sempere, P.S.J. Russell, Optical properties of photonic crystal fiber with integral micron-sized Ge wire. *Opt. Express* **16**(22), 17227–17236 (2008)
11. H.W. Lee, M.A. Schmidt, H.K. Tyagi, L.P. Sempere, P.S.J. Russell, Polarization-dependent coupling to plasmon modes on submicron gold wire in photonic crystal fiber. *Appl. Phys. Lett.* **93**(11), 111102 (2008)
12. A. Nagasaki, K. Saitoh, M. Koshiba, Polarization characteristics of photonic crystal fibers selectively filled with metal wires into cladding air holes. *Opt. Express* **19**(4), 3799–3808 (2011)
13. M.F. Sultan, A.A. Al-Zuky, S.A. Kadhim, Performance parameters evaluation of surface plasmon resonance based fiber optic sensor with different bilayer metals: theoretical study. *Al-Mustansiriyah J. Sci.* **29**(1), 195–203 (2018)
14. E. Wijaya, C. Lenaerts, S. Maricot, J. Hastanin, S. Habraken, J.P. Vilcot, S. Szunerits, Surface plasmon resonance-based biosensors: from the development of different SPR structures to novel surface functionalization strategies. *Curr. Opin. Solid State Mater. Sci.* **15**(5), 208–224 (2011)
15. G.Y. Oh, T.K. Lee, H.S. Kim, D.G. Kim, Y.W. Choi, Design of ultra-sensitive biosensor applying surface plasmon resonance to a triangular resonator. *Opt. Express* **20**(17), 19067–19074 (2012)

16. V. Koubova, E. Brynda, L. Karasova, J. Škvor, J. Homola, J. Dostalek, J. Rošický, Detection of foodborne pathogens using surface plasmon resonance biosensors. *Sens. Actuators, B Chem.* **74**(1–3), 100–105 (2001)
17. J. Homola, J. Dostalek, S. Chen, A. Rasooly, S. Jiang, S.S. Yee, Spectral surface plasmon resonance biosensor for detection of staphylococcal enterotoxin B in milk. *Int. J. Food Microbiol.* **75**(1–2), 61–69 (2002)
18. N. Chen, M. Chang, X. Zhang, J. Zhou, X. Lu, S. Zhuang, Highly sensitive plasmonic sensor based on a dual-side polished photonic crystal fiber for component content sensing applications. *Nanomaterials* **9**(11), 1587 (2019)
19. J.H. Osório, J.G. Hayashi, Y.A. Espinel, M.A. Franco, M.V. Andrés, C.M. Cordeiro, Photonic-crystal fiber-based pressure sensor for dual environment monitoring. *Appl. Opt.* **53**(17), 3668–3672 (2014)
20. T.T. Goodrich, H.J. Lee, R.M. Corn, Direct detection of genomic DNA by enzymatically amplified SPR imaging measurements of RNA microarrays. *J. Am. Chem. Soc.* **126**(13), 4086–4087 (2004)
21. V. Marquez-Cruz, J. Albert, High resolution NIR TFBG-assisted biochemical sensors. *J. Lightwave Technol.* **33**(16), 3363–3373 (2015)
22. M. Batumalay, S.W. Harun, F. Ahmad, R.M. Nor, N.R. Zulkepely, H. Ahmad, Study of a fiber optic humidity sensor based on agarose gel. *J. Mod. Opt.* **61**(3), 244–248 (2014)
23. L. Zhang, F. Gu, J. Lou, X. Yin, L. Tong, Fast detection of humidity with a subwavelength-diameter fiber taper coated with gelatin film. *Opt. Express* **16**(17), 13349–13353 (2008)
24. W. Xie, M. Yang, Y. Cheng, D. Li, Y. Zhang, Z. Zhuang, Optical fiber relative-humidity sensor with evaporated dielectric coatings on fiber end-face. *Opt. Fiber Technol.* **20**(4), 314–319 (2014)
25. X. Liu, M. Jiang, Q. Sui, X. Geng, Optical fibre Fabry–Perot relative humidity sensor based on HCPCF and chitosan film. *J. Mod. Opt.* **63**(17), 1668–1674 (2016)
26. J.S. Sirkis, D.D. Brennan, M.A. Putman, T.A. Berkoff, A.D. Kersey, E.J. Friebele, In-line fiber etalon for strain measurement. *Opt. Lett.* **18**(22), 1973–1975 (1993)
27. F.L. Pedrotti, L.S. Pedrotti, L.M. Pedrotti, *Introduction to optics* (Pearson, London, 2007)
28. W.H. Tsai, C.J. Lin, A novel structure for the intrinsic Fabry–Perot fiber-optic temperature sensor. *J. Lightwave Technol.* **19**(5), 682–686 (2001)
29. S.H. Kim, J.J. Lee, D.C. Lee, I.B. Kwon, A study on the development of transmission-type extrinsic Fabry–Perot interferometric optical fiber sensor. *J. Lightw. Technol.* **17**, 1869–1874 (1999)
30. J.R. Zhao, X.G. Huang, W.X. He, J.H. Chen, High-resolution and temperature-insensitive fiber optic refractive index sensor based on fresnel reflection modulated by Fabry–Perot interference. *J. Lightw. Technol.* **28**, 2799–2803 (2010)
31. P. Morris, A. Hurrell, A. Shaw, E. Zhang, P. Beard, A Fabry–Perot fiber-optic ultrasonic hydrophone for the simultaneous measurement of temperature and acoustic pressure. *J. Acoust. Soc. Am.* **125**, 3611–3622 (2009)
32. Y. Zhang, X. Chen, Y. Wang, K.L. Cooper, A. Wang, Microgap multicavity Fabry–Pérot biosensor. *J. Lightw. Technol.* **25**, 1797–1804 (2007)
33. V.R. Machavaram, R.A. Badcock, G.F. Fernando, Fabrication of intrinsic fibre Fabry–Perot sensors in silica fibers using hydrofluoric acid etching. *Sen. Actuat. A* **138**, 248–260 (2007)
34. X. Wan, H.F. Taylor, Intrinsic fiber Fabry–Perot temperature sensor with fiber Bragg grating mirrors. *Opt. Lett.* **27**, 1388–1390 (2002)
35. Z. Wang, F. Shen, L. Song, X. Wang, A. Wang, Multiplexed fiber Fabry–Pérot interferometer sensors based on ultrashort Bragg gratings. *IEEE Photon. Technol. Lett.* **19**, 622–624 (2007)
36. D.J.J. Hu, R.Y.N. Wong, P.P. Shum, Photonic crystal fiber-based interferometric sensors. Selected topics on optical fiber technologies and applications, pp. 21–41 (2018). <https://doi.org/10.5772/intechopen.70713>

Publisher’s Note Springer Nature remains neutral with regard to jurisdictional claims in published maps and institutional affiliations.

Springer Nature or its licensor (e.g. a society or other partner) holds exclusive rights to this article under a publishing agreement with the author(s) or other rightsholder(s); author self-archiving of the accepted manuscript version of this article is solely governed by the terms of such publishing agreement and applicable law.